Curvature-Driven Min/Max Flow and Anisotropic Diffusion in Image Enhancement

Andrew P. Papliński*
Computer Science and Software Engineering, Monash University, Australia
app@csse.monash.edu.au

Abstract

We compare application of two partial differential equation methods in image enhancement. The first method is based on the curvature-driven min/max flow and originates from the level set methods. The second method is an anisotropy diffusion flow. The curvature-driven method seems to enhance better the significant edges in the image, whereas the anisotropic diffusion seems to work better with smoothing intra-regional image features.

1 Introduction

In this work we compare two non-linear methods of image enhancement based on application of partial differential equations, namely, the curvature-driven min/max flow [1, 2] and an anisotropy diffusion method [3]. Comprehensive bibliography on variational methods can be found in [**?**] and [2]. By image enhancement we understand processing of an image in such a way to maintain or possibly enhance sharp edges of an image and to remove small intra-regional features considered to be noise, that is, to smooth intensity inside image regions. This work originated from our work presented in [4, 5] on application of partial differential equations in interpretation of the Posterior Capsular Opacification images [9, 10, **?**].

2 Curvature-Driven Min/Max Flow

The curvature-driven evolution of an image $u(\mathbf{x}, t)$ is described by the following partial differential equation [2]:

$$\frac{\partial u(\mathbf{x},t)}{\partial t} = F(\kappa(\mathbf{x},t))|\nabla u(\mathbf{x},t)| \ , \quad \kappa = \text{div}(\frac{\nabla u}{|\nabla u|}) \tag{1}$$

where $u(\mathbf{x}, t)$ is an evolving image intensity, ∇u is its gradient, and $F(\kappa)$ is an appropriately selected "speed" function of the image curvature, κ.

Early examples of the speed functions are considered, among others, in [11] where $F = \kappa$, and in [12] where $F = \kappa^{1/3}$. In each of this schemes, all image information would be eventually filtered out if iterations are performed continuously. This is the result of the Grayson's theorem [13, 14] which says that each contour shrinks to zero and disappears.

*This paper was prepared with the financial support of the Electrical & Computer Engineering Department and the NASA ACE Center, the University of New Mexico

An elegant way to address this problem is a min/max flow method introduced in [1, 2]. Under the min/max principle the speed function, $F(\kappa)$, is of the following form

$$F(\kappa(\mathbf{x})) = \begin{cases} \max(\kappa, 0) & \text{if } \text{ave}_\rho(u(\mathbf{x})) < \text{ave}_\perp(u(\mathbf{x})) \\ \min(\kappa, 0) & \text{otherwise} \end{cases} \tag{2}$$

where $\text{ave}_\rho(u(\mathbf{x}))$ is an average intensity in the neighborhood of a pixel $\mathbf{x}$ of a radius ρ, and $\text{ave}_\perp(u(\mathbf{x}))$ is an average intensity on the direction perpendicular to the gradient, that is, tangent to the iso-intensity contour line. It can be observed [1, 2] that flow under $F = \max(\kappa, 0)$ (positive-only curvature) smoothes away all image details, whereas, flow driven by $F = \min(\kappa, 0)$ (negative-only curvature) preserves the strong edges of the image.

The average intensity in the neighborhood of a pixel $\mathbf{x}$ of a radius ρ, $\text{ave}_\perp(u(\mathbf{x}))$, is calculated as a convolution of the evolving image, $u(\mathbf{x})$, with a $\rho \times \rho$ Gaussian mask of the variance $\sigma^2 = 0.5\rho^2$. Increasing the radius, ρ, the amount of smoothing is in general increased.

In order to calculate the average intensity along the line tangent to the iso-intensity contour we first note that such a tangent line can, in general, go in between the image pixels. Therefore, in the average we include intensities at the pixels located at a strip of a given width around the tangent line. The intensities are weighted with the distance from the tangent line, which can be calculated as the projection of the location vector, $\mathbf{x}$, on the gradient, ∇u. The average is taken only on the segment of the tangent line inside the disk of the radius ρ.

The min/max flow as described by eqns (1), (2) is applied to a test image which is a 120×130-pixel section of the alumgrns (aluminum grains) image distorted with a 10% uniform noise. The original noisy image and an image after 40 iterations are shown in Figure 1.

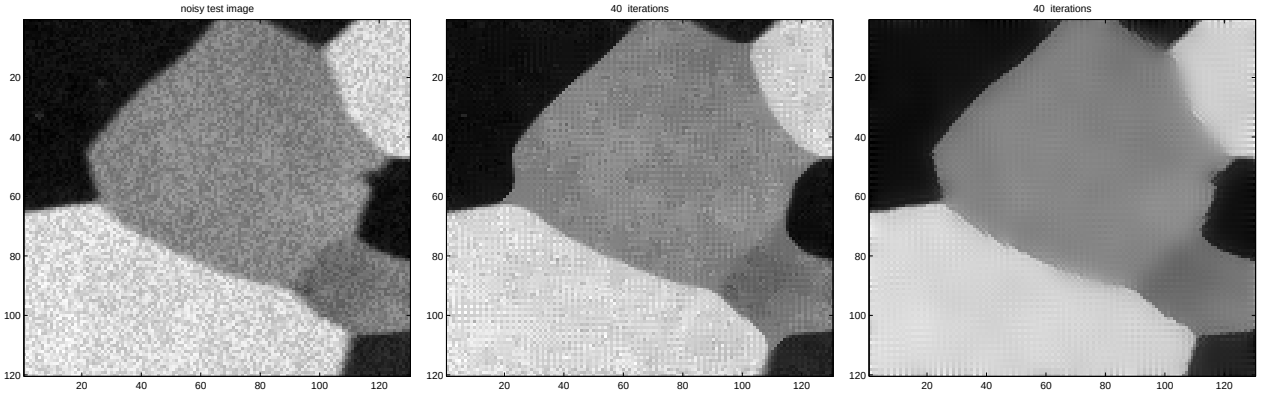

a b c

Figure 1: The original noisy image (a), the image after 40 iterations using the min/max flow (b) and the anisotropic diffusion (c).

From Figure 1 b it can be noticed that the borders between areas of unified intensity have been enhanced, and the noise from inside the image regions has been filtered out. The enhancement of the region borders occurs through their thinning and averaging their curvatures. The degree of smoothing is controlled by the radius of the averaging disk, ρ.

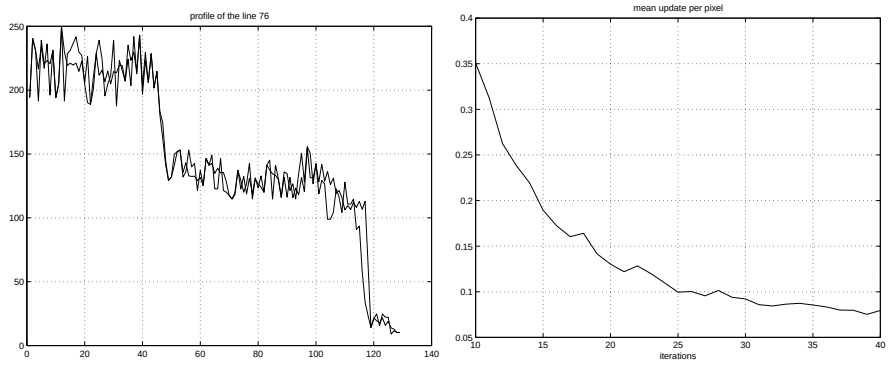

Figure 2: Left: The profile of the line 78. Right: The mean update per pixel during iterations

Some additional features of the max/min curvature flow can be observed from Figure 2 where a cross-section of the image intensity along the specified line has been shown. Note that the large gradient has been increased by increasing the slope of the line. This is equivalent to the thinning an image region. Small variations of the gradient have been non-linearly averaged. It is also important to note from the right plot in Figure 2 that the mean update per pixel is being exponentially reduced which demonstrates the convergence of the algorithm.

3 Anisotropic diffusion method

An anisotropic diffusion equation is similar to the previously considered curvature-based equation in that that it is also comprised of only first and second spatial derivatives, and that it is also a nonlinear partial differential equation. A standard form of an anisotropic diffusion equation is as follow:

$$\frac{\partial u(\mathbf{x},t)}{\partial t} = \text{div}(L(\mathbf{x},t)\nabla u(\mathbf{x},t)) \tag{3}$$

where $L(\mathbf{x},t)$ is a 2×2 diffusion matrix controlling anisotropy. In a special case when the anisotropy matrix is identity, eqn (3) describes isotropic diffusion which in terms of the image processing smoothes all image features away. The anisotropic diffusion equation describes image changes which are proportional to the sum of spatial derivatives of the diffusion vector, $v = L \cdot \nabla u$. In particular, when the diffusion vector becomes zero, the image intensity reaches its steady state and the image pixel remains unchanged. Note that the diffusion vector, v, becomes zero when either the gradient is zero, or the diffusion matrix is the orthogonal projection of the gradient.

Following [3] we exploit two basic ideas which are important from the point of view of obtaining image enhancement behaviour of the algorithm based on eqn (3). The first idea is that the anisotropy vector should steadily reach the value of zero, and the second one is that such a state should be obtained either by the diffusion matrix being the orthogonal projection of the image gradient which gives $v = L \cdot \nabla u = 0$, or by the image gradient approaching zero. This can be achieved by means of the following relaxation equation for the anisotropy matrix:

$$\frac{\partial L(\mathbf{x},t)}{\partial t} + \frac{1}{\tau}L(\mathbf{x},t) = \frac{1}{\tau}F(\nabla u(\mathbf{x},t)) \tag{4}$$

where $F(\nabla u(\mathbf{x}, t))$ is a 2×2 anisotropy "force" matrix, and τ is a time constant which determines the speed of relaxation of the diffusion matrix. Eqn (4) describes evolution of the diffusion matrix from its initial value, say $L = I$ to the one which is enforced by the F matrix. The specific form of the force matrix, F, will be selected based on the value of of the magnitude of the image gradient. If the image gradient exceeds a threshold parameter, s, then the matrix F will be the orthogonal projection of the gradient, otherwise its form will ensure isotropic diffusion, which smoothes the image in the areas where the gradient falls below the threshold parameter. Details are presented in [**?**]

The set of equations (3), (4) gives a stable solution to the anisotropic diffusion equation which ensures maintaining strong edges in the image and flattening image features which are considered to be irrelevant. For a rigorous mathematical treatment the reader is referred to [3].

The results of processing the test image are presented in Figure 1 c. From Figure 1 c it can be observed that the borders between image regions considered to be significant with respect to the stiffness threshold, s, have been maintained, whereas, the intra-regional features have been strongly filtered out. This results in a segmentation-like processing of an image. Some additional aspects of the anisotropic diffusion iterations have been presented in Figure 3.

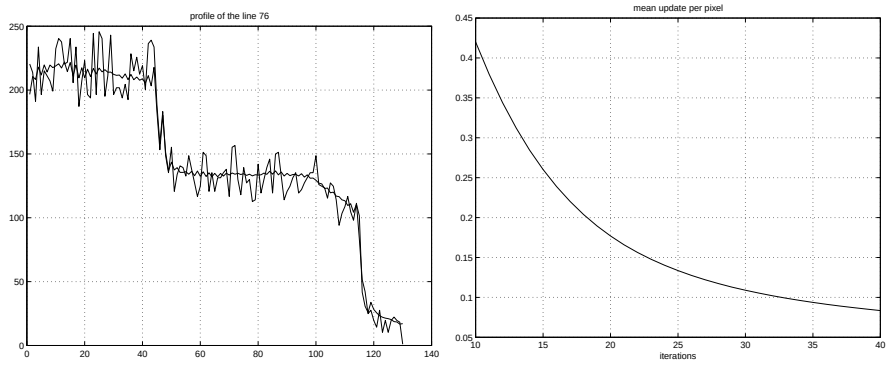

Figure 3: Left: The profile of the line 78. Right: The mean update per pixel during iterations

From Figure 3 it can be noticed that for the selected parameters β and τ low-pass filtering is very prominent. The convergence of the algorithm characterised by the mean update per pixel is similar to that of the curvature driven min/max flow.

Comparing the curvature driven min/max flow and the anisotropic diffusion we can note that the first method actively enhances the inter-regional borders by modifying the curvature of the border curves. The second method appears to be better in filtering out the intra-regional features. Both algorithms maintain the average values of the image intensity, which is a very convenient feature, and converge to a steady-state.

Concluding remarks

The method which combines the curvature-driven min/max flow and anisotropic diffusion takes advantage of the best aspects of two constituent methods. In particular, the curvature-driven method seems to enhance better the significant edges in the image, whereas the anisotropic diffusion seems to work better with smoothing intra-regional image features.

References

[1] R. Malladi and J. A. Sethian, "Image processing: Flows under min/max curvature and mean curvature," *Graphical Models and Image Processing*, vol. 58, no. 2, pp. 127–141, 1996.

[2] J. A. Sethian, *Level Set Methods and Fast Marching Methods*. Cambridge University Press, 2nd ed., 1999.

[3] G. H. Cottet and M. El Ayyadi, "A Voltera type model for image processing," *IEEE Transactions on Image Processing*, vol. 7, pp. 292–303, March 1998.

[4] A. P. Papliński and J. F. Boyce, "Processing a class of ophthalmological images using an anisotropic diffusion equation," in *Proceedings of the 2nd Annual IASTED International Conference on Computer Graphics and Imaging (CGIM'99)*, (Palm Springs, California, USA), pp. 134–138, October 1999.

[5] A. P. Papliński and J. F. Boyce, "Application of an anisotropic diffusion equation in processing a class of ophthalmological images," in *Proceedings of the International Symposium on Advanced Concepts for Intelligent Vision Systems (ACIVS'99)*, (Baden-Baden, Germany), pp. 33–39, The International Institute for Advanced Studies in Systems Research and Cybernetics, August 1999.

[6] S. A. Barman, J. F. Boyce, D. J. Spalton, P. G. Ursell, and E. J. Hollick, "Measurement of posterior capsule opacification," in *Proceedings of the Conference on Medical Image Understanding and Analysis, MIUA97*, July 1997. Oxford, U.K.

[7] M. V. Pande, P. G. Ursell, D. J. Spalton, and S. Kundaiker, "High resolution digital retroillumination imaging of the posterior lens capsule after cataract surgery," *J. Cataract Refract. Surg.*, vol. 23, pp. 1521–1527, 1997.

[8] D. S. Friedman, D. D. Duncan, M. Beatriz, and S. K. West, "Digital image capture and automated analysis of posterior capsular opacification," *Invest. Ophthalmology Vis. Sci.*, vol. 40, pp. 1715–1726, July 1999.

[9] A. P. Papliński and J. F. Boyce, "Segmentation of a class of ophthalmological images using a directional variance operator and co-occurrence arrays," *Optical Engineering*, vol. 36, pp. 3140–3147, November 1997.

[10] A. P. Papliński, "Directional filtering in edge detection," *IEEE Trans. Image Proc.*, vol. 7, pp. 611–615, April 1998.

[11] L. Alvarez and L. Mazorra, "Image selective smoothing and edge detection by non-liner diffusion," *SIAM J. Num. Anal.*, vol. 29, no. 3, pp. 845–866, 1992.

[12] G. Sapiro and A. Tannenbaum, "Image smoothing based on affine invariant flow," in *Proceedings of the Conference on Information Sciences and Systems*, (Johns Hopkins University), March 1993.

[13] M. Grayson, "The heat equation shrinks embedded plane curves to round points," *J. Diff. Geom.*, no. 26, p. 285, 1987.

[14] M. Grayson, "A short note on the evolution of surfaces via mean curvatures," *J. Diff. Geom.*, p. 555, 1989.